14

# Intersublevel Relaxation Properties of Self-Assembled InAs/GaAs Quantum Dot Heterostructures

[1]Jiunn-Chyi Lee and [2]Ya-Fen Wu
[1]*Electrical Engineering, Technology and Science Institute of Northern Taiwan*
[2]*Electronic Engineering, Ming Chi University of Technology*
*Taiwan*

## 1. Introduction

The requirement for high performance optoelectronic devices has spurred much experimental effort directed toward understanding and exploiting the electronic and optical properties of quantum dots (QDs). The relaxation dynamics in the zero-dimensional QD systems is expected to differ qualitatively from higher-dimensional systems, since the density of states is a series of $\delta$-functions. The limited number of states available for carriers impairs carrier relaxation toward the ground state (phonon bottleneck effect) (Benisty et al., 1991; Benisty, 1995; Hai et al., 2006). In addition, the finite degeneracy of each QD state leads already to state filling effects when few carriers populate the lowest dot states. Both effects possibly result in intersublevel relaxation rates that are comparable to interband recombination rates and have been used to explain observed photoluminescence (PL) from excited states of QDs (Bissiri et al., 2001; Smith et al., 2001).
The temperature dependence of PL emissions has been the subject of extensive studies for clarifying the mechanism of PL quenching processes in a randomly distributed dot structure (Bafna et al., 2006; Duarte et al., 2003; Polimeni et al., 1999). The PL spectra of QDs typically show peculiar temperature dependencies. A large temperature induced peak energy decrease, which is eventually sigmoidal, and a reduction of the PL full width at half maximum (FWHM) in mid-temperature range, have been reported (Dawson et al., 2005; Polimeni et al., 1999). The phenomenon is commonly attributed to effectively redistributed carriers in QDs through the channel of the wetting layer based on a model of the temperature driven carrier dynamics which takes into account the QD size distribution, random population, and carrier capture relaxation and retrapping (Nee et al., 2005; Nee et al., 2006). The physics of carrier relaxing between intersublevels in various QD systems has been extensively studied. However, the electron-phonon scattering effect on QD system is neglected and only considered in the high-temperature range to explain the increase of FWHM (Dawson et al., 2005; Nee et al., 2005; Nee et al., 2006), and the effect of dot size, density, and uniformity on this mechanism is still not fully understood (Dawson et al., 2005; Duarte et al., 2003).

In this chapter, we studied the phonon-assisted transferring of carriers in InAs QD system via an analysis of PL data in the temperature range from 15 K to 280 K. Intersublevel relaxation properties and thermally-induced activation of excitons in QD system are simulated using a rate-equation model based on carrier relaxation and thermal emission in the quantum dot system. The dot-size distribution, thermal escaping and retrapping, and electron-phonon scattering, are all considered in the model. Correlation between carrier redistribution and electron-phonon scattering effects is quantitatively discussed to explain the different temperature-dependent behaviors of the PL spectra measured from samples with different dot size distribution. Moreover, the phonon-bottleneck effect on temperature dependent PL spectra is also discussed to illustrate the significance of phonon-assisted effect on QD system. According to the simulation results, intersublevel relaxation lifetimes of QD samples are estimated under different temperatures and the carrier transferring mechanisms in the QD system are discussed in detail. The theoretical analysis confirms that the thermal redistribution of carriers and the electron phonon scattering affect the temperature dependent PL spectra simultaneously.

## 2. Sample Preparation

An easy way to fabricate zero-dimensional InAs QDs is to grow the InAs on GaAs in the S-K mode (Sanguinetti et al, 2002; Schmidt et al., 1996). In the S-K transformation, growth is initially two-dimensional, until the film reaches a strain dependent critical thickness. Above the critical deposition thickness of InAs on GaAs substrate, due to the 7% lattice mismatch between GaAs and InAs, the two-dimensional growth changes into a three-dimensional one. Coherent InAs islands with lateral extensions of 10-20 nm are spontaneously formed on top of the two-dimensional layer, called the wetting layer. It was traditionally believed that islands formed in S-K growth are dislocated. However, the experiment on InAs/GaAs (001) has demonstrated the formation of three-dimensional coherently strained islands.

The self-assembled InAs QD samples used in the work were created by using a metal-organic chemical vapor epitaxy system (MOCVD) system. The substrates were (100) 2°-tilted toward (111)A Si-doped GaAs. The heterostructures included a 400 nm Si-doped GaAs buffer layer, an InAs QD active region of 3 monolayers (MLs) and a 100 nm undoped GaAs capping layer. The growth rate was 0.1 MLs and the V/III ratio during the growth of InAs layer was 6.36 for samples A, B and 3 for sample C. The growth interruption (GI) introduced during dot formation for samples A, B, and C were set to 6 s, 15 s and 15 s, respectively. In order to investigate the average dot size distribution and shape, images of these samples were taken by high-resolution transmission electron microscopy (HRTEM) operating at 200 keV. PL measurements were carried out under the excitation of a continuous-wave He-Cd laser emitting at 325 nm, with the incident power intensity being 20 mW. The samples were mounted in a closed cycle He cryostat, which allowed measurements in a temperature ($T$) range from 15 K to 280 K. The luminescence was dispersed in a 0.5 meter monochromator, and detected with a Ge photodiode using a standard lock-in technique.

Figure 1 shows the plan-view TEM images for samples A, B and C. The quantitative data on size distribution of the InAs QD samples have been obtained from the TEM images, the average dot density of samples A, B and C are $2.4\times10^{10}$ cm$^{-2}$, $1.2\times10^{10}$ cm$^{-2}$ and $1.4\times10^{10}$ cm$^{-2}$, respectively, and the average dot diameters of the three samples are 16 nm, 19 nm and 20 nm. Generally, the application of GI time results in the formation of larger sized QDs with a

regular size distribution (Tarasov et al., 2000), as can be seen from Fig. 1(a) and Fig. 1(b). Besides, decreasing the V/III ratio during growth can increase the indium adatom surface diffusivity in the wetting layer and hence increasing the two-dimensional island size in the wetting layer. A layer composed of larger two-dimensional islands will have a more uniform strain distribution and lead to a more uniform island distribution on top of the wetting layer (Solomon et al., 1995). The highest uniformity was exhibited for sample C as can be seen in Fig. 1(c).

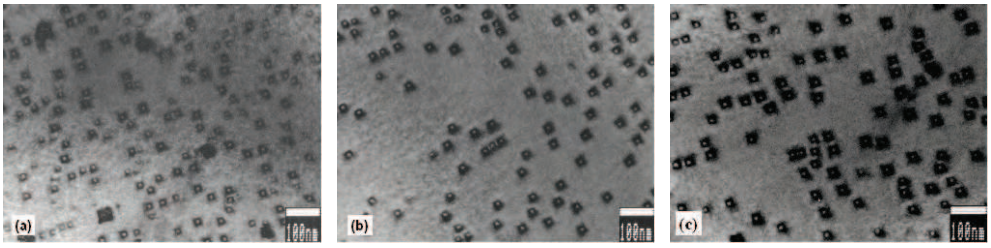


Fig. 1. Plan-view TEM images of the InAs quantum dots of (a) sample A, (b) sample B, and (c) sample C

## 3. Results and Discussions

### 3.1 Photoluminescence Characterization

The measured PL spectra at temperature $T$=15 K for the samples are shown in Fig. 2. All of these spectra exhibit a pronounced double-like feature and can be decomposed into two Gaussian peaks; we attribute these two main spectral features of the QDs to the ground state and excited state emissions. Sample A possesses the largest ground state and excited state transmission energies, i.e., 1.05 eV and 1.11 eV; and the values are 1.01 eV, 1.09 eV and 1.01 eV, 1.08 eV for sample B and sample C, respectively. Considering the quantum-size effect on the peak energies, we believe that the excitons localized in smaller dots will contribute to higher peak energies (Cheng et al., 1998). As a result, the highest peak energies of sample A (GI=6s) is attributed to the smallest size of the QDs in the three samples. Similarly, the peak energies for sample B and sample C are almost the same because their dot sizes are similar.

One remarkable feature in Fig. 2 is the obvious difference of the excited state peak intensities among the samples. The strongest excited state peak intensity of sample A reveals that more carriers exists in this state, and the much weaker excited state emissions in PL intensity of sample C suggests that the carriers relax rapidly into the ground state. In other words, it has shorter relaxation lifetimes than those of sample A and sample B. It indicates for sample C a restricted phonon bottleneck effect (Benisty et al., 1991; Bockelmann et al. 1990). This can be understood in terms of an improved confinement of InAs excitons and a lower defect density in sample C due to having best uniformity among the three samples.

The values of FWHM of ground state and excited state emissions are 27.1 meV and 88.3 meV for sample A, 26.8 meV and 79.6 meV for sample B, and for sample C they are 23.3 meV and 55.27 meV, respectively. The PL linewidth is mainly determined by the inhomogeneous broadening of InAs islands resulted from size fluctuation of the dot size at low temperature (Xu et al.,1996), the measured data for sample C are consistent with its better size uniformity.

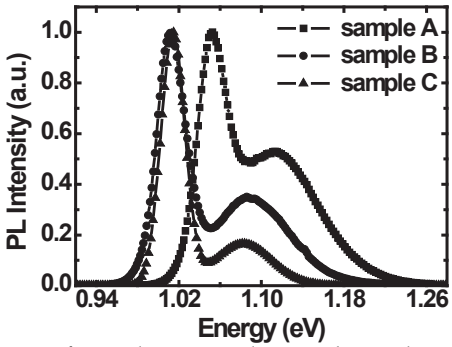


Fig. 2. Normalized PL spectra of sample A, sample B, and sample C recorded at $T$=15 K. The excitation energy is 20 mW

The two-dimensional contour plots in Fig. 3 display the measured temperature dependent PL intensities. The distributions of emission energy from the QD systems are clearly seen from the figures. Sample A has the widest emission band, luminescence from the excited state is apparent. The narrowest energy spreading is the contour shown for sample C. The PL intensity of excited state is too small to be observable and the PL spectra are concentrated in a narrow linewidth. Since the observation of PL from excited states transition at low

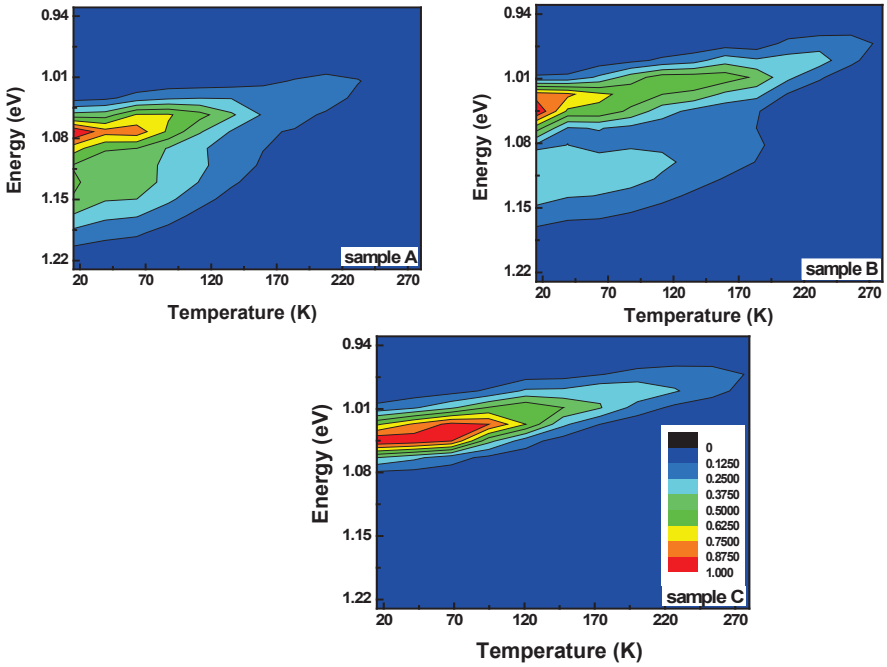


Fig. 3. Two-dimensional contour plots of the PL intensities for sample A, sample B, and sample C, measured in the temperature range from 15 to 280 K

excitation density is explained by the phonon bottleneck effect in the QD system, we attribute the inconspicuous excited state emission of sample C to the partially relaxed phonon bottleneck.

Figure 4(a) displays the temperature dependent FWHMs of PL spectra of the samples, both the ground state and the excited state are included. Observing the FWHMs of sample A and sample B, they stay constant up to 75 K and 100 K. As the temperature further increases, anomalous reduction appeared within the temperature range from 100 K to 200 K. The FWHMs decrease and the minimal FWHMs of excited state are found to be around 69 meV at 200 K for both samples. When the temperature is higher than 200 K, the PL linewidths start to increase with temperature. At low temperature, carriers are captured randomly into the QDs. With increasing temperature, carriers are thermally activated outside the dots with shallow energy minima into the wetting layer then retrapped into another dot. Carrier hopping among dots favors a drift of carriers towards the dots with lower energy emissions and leading to the decrease of FWHMs. As temperature exceeds 200 K, the FWHMs increase with temperature because the electron-phonon scattering becomes important. Figure 4(b) shows the PL excited state peak energy with increasing temperature, and the corresponding values of InAs band gap using Varshni law with the InAs parameters are also shown. As can be seen in the figure, the redshift of emission peaks for sample A and B are faster than that of the InAs bulk band gap at $T$=100-200 K, coincided with the carrier hopping mechanism described above.

Significantly different temperature dependent FWHMs are observed for sample C. The broadening of the PL spectra exhibits no reduction as the temperature increases, but the peak energy shifts with a slight sigmoid dependence on temperature. Thanks to the lowest PL intensity of excited state, fewer carriers exist in the state, and the thermal redistribution of carriers via wetting layer is indistinct. The slightly quick redshift of peak energy is consistent with the weak redistribution effect, whereas the increase of linewidth with temperature implies that the electron-phonon scattering is dominant in the PL spectra. Therefore, to analyze the carriers transferring mechanisms, we investigate a model for carrier dynamics in QD system under optical excitation which includes the thermal redistribution effect and the electron-phonon scattering effect.

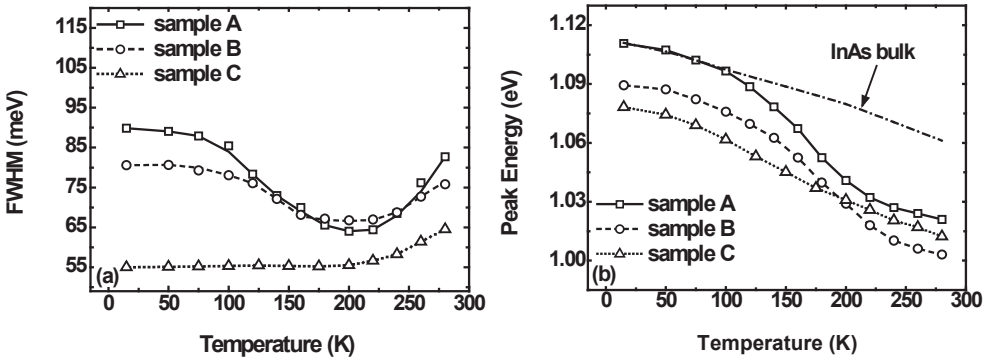


Fig. 4. Experimental values of the temperature dependent (a) FWHM and (b) peak energy of the excited state of sample A, sample B, and sample C

### 3.2 Theoretical Model

The possible optical transitions in a single QD consist of a series of $\delta$ function lines, whose energy positions depend on the particular three-dimensionality confined levels. In a real QD ensemble each individual dots are slightly different in size, shape, strain state, etc. The main impact of size fluctuations is a variation in the energy position of electronic levels, and subsequently to an inhomogeneous broadening of the ensemble properties. It is reasonable to assume a Gaussian distribution for it (Chang et al., 1999).

To analyze the carrier dynamics of the QD system, we develop a theoretical model that takes into account the QDs size distribution, the state filling effect, and all of the important carrier transport processes, including the carrier capture and relaxation, thermal emission and retrapping, and radiative and nonradiative recombination. Referring to the model of the QD system described schematically in Fig. 5, four discrete levels of electron (labeled as $i$, $i$=1-4) are considered in the system, namely, the ground state ($E_1$), the excited state ($E_2$), the wetting layer ($E_3$), and the GaAs barrier ($E_4$). Since the process of quantum dot population is intrinsically random, the density of states for both ground state [$n_1(E)$] and excited state [$n_2(E)$] are assumed to be proportional to their Gaussian distributions, with parameters chosen to match the peak energies and linewidths of the lowest temperature PL spectra (Lee et al., 1997; Yang et al., 1997) and taking spin into consideration, then

$$\int n_i(E)dE = \int \left[ n_{if}(E) + n_{ie}(E) \right] dE \propto 2 \times i \times n_d \,, \tag{1}$$

where $i$=1, 2; $n_{if}$ and $n_{ie}$ are the filled and empty energy states of the $i$-th level, respectively, and $n_d$ is the dot density of the sample.

The carrier dynamics taken into account in this model are described as follows. First, the coupling among those four carrier reservoirs is treated as a relaxation ladder process from each energy level to its lower level neighbor. Carriers are injected from the GaAs barrier into the wetting layer at rate $g$, from where they are captured into the excited state of QDs within a capture time $\tau_{32}$. Further on, carriers in the excited state relax to the ground state in a time of $\tau_{21}$ or radiatively recombine. The relaxation lifetime of one electron in the $i$-th level ($\tau_{i,i\text{-}1}$) is proportional to the filling ratio of the ($i$−1)-th level ($f_{i-1}$), and expressed as (Mukai et al., 1996)

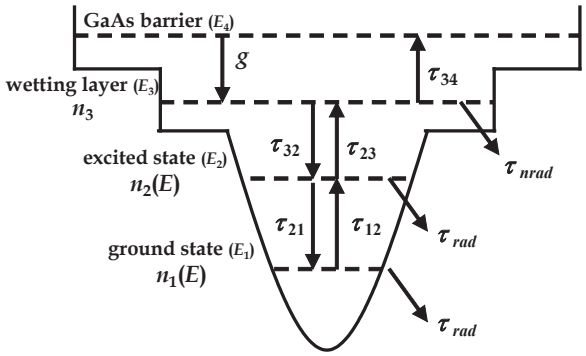


Fig. 5. Schematic representation of the processes taken into account in the rate equation model

$$\tau_{i,i-1} = \tau_{i,i-1,0} \times \left(1 - f_{i-1}\right)^{-1},\ i = 2, 3, \tag{2}$$

where $\tau_{i,i\text{-}1,0}$ is the intrinsic relaxation lifetime.
Secondly, thermal emission of the carriers toward an adjacent higher energy level arises when the temperature is sufficiently high. The coefficients corresponding to emitting from the ground state to the excited state, the excited state to the wetting layer, and the wetting layer to the GaAs barrier are given by $\tau_{12}$, $\tau_{23}$, and $\tau_{34}$, respectively. In QD systems, the thermal emission and retrapping of carriers in the excited state via the wetting layer is a typical explanation for the unusual decrease of PL linewidth in the mid-temperature range (Lobo et al., 1999; Polimeni et al., 1999; Giorgi et al., 2001). We express the thermal emission time of the $i$-th level as $\tau_{i,i+1}$, and

$$\tau_{i,i+1} = \tau_{i,i+1,0} \times \exp\left[\left(E_{i+1} - E_i\right)/kT\right],\ i = 1, 2, 3, \tag{3}$$

where $\tau_{i,i+1,0}$ is the intrinsic thermal emission lifetime of level $i$. Since the peak interval between the ground state and the excited state is much larger than the value of $kT$, the thermal emission from ground state to excited state is neglected in our model.
The third type of carrier dynamics considered in this system is the radiative recombination. We have neglected any recombination from the second excited state of the dots, since no PL is observed at energies possible for the second excited state, and assumed that only two discrete electron levels exist inside a quantum dot, i.e., the ground state and the first excited state. The radiative recombination lifetime $\tau_{rad}$ is assumed to be the same for both of the states in all of the QDs and is constant with respect to $T$.
The system under steady-state conditions is then characterized by the following equations: (Lee et al., 2008; Sanguinetti et al., 1999; Wu et al., 2008)

$$\frac{dn_3}{dt} = g - \int \frac{n_3}{\tau_{32}} \times \frac{n_{2e}(E)}{n_2(E)} dE + \int \frac{n_{2f}(E)}{\tau_{23}} dE - \frac{n_3}{\tau_{34}} - \frac{n_3}{\tau_{nrad}} = 0, \tag{4}$$

$$\frac{dn_{2f}(E)}{dt} = \frac{n_3}{\tau_{32}} \times \frac{n_{2e}(E)}{n_2(E)} - \frac{n_{2f}(E)}{\tau_{21}} \times \frac{n_{1e}(E)}{n_1(E)} + \frac{n_{1f}(E)}{\tau_{12}} \times \frac{n_{2e}(E)}{n_2(E)} - \frac{n_{2f}(E)}{\tau_{23}} - \frac{n_{2f}(E)}{\tau_{rad}} = 0, \tag{5}$$

$$\frac{dn_{1f}(E)}{dt} = \frac{n_{2f}(E)}{\tau_{21}} \times \frac{n_{1e}(E)}{n_1(E)} - \frac{n_{1f}(E)}{\tau_{12}} \times \frac{n_{2e}(E)}{n_2(E)} - \frac{n_{1f}(E)}{\tau_{rad}} = 0. \tag{6}$$

The last term in (4) is the nonradiative loss of excitons in wetting layer, and $\tau_{nrad}$ is the nonradiative recombination lifetime. The state filling effect is essentially significant in the QD system because of the reduced density of states and should be taken into account. Prior to the description of the simulation process, we must discuss the parameters used in the model. To obtain $\tau_{rad}$ used in our model, we estimate the intrinsic exciton lifetime in QDs ($\tau_{QD}$) at low temperature in terms of the exciton lifetime in a corresponding quantum well ($\tau_{QW}$) by (Malik et al., 2001)

$$\tau_{QD} = \frac{3}{2}\tau_{QW}\left(\frac{\eta}{k_{ex}}\right)^2 . \tag{7}$$

Here $k_{ex}=2\pi n/\lambda_{PL}$ is the reciprocal wavelength of the emitted light in the quantum dot material, with the refractive index of InAs, and $\eta$ is a measure of the lateral dot size. By using values of $\eta=(1/15)$ nm$^{-1}$, $n=3.6$, $\lambda_{PL}=1181$ nm, and an exciton lifetime $\tau_{WL}$ of 25 ps, the radiative recombination lifetime $\tau_{rad}$ is calculated to be approximately 500 ps and assumed to be independent from temperatures.
Rewrite (4), (5) and (6) at $T=15$ K where the thermal emission can be neglected:

$$\frac{dn_3}{dt} = g - \int \frac{n_3}{\tau_{32}} \times \frac{n_{2e}(E)}{n_2(E)} dE - \frac{n_3}{\tau_{nrad}} = 0 , \tag{8}$$

$$\frac{dn_{2f}(E)}{dt} = \frac{n_3}{\tau_{32}} \times \frac{n_{2e}(E)}{n_2(E)} - \frac{n_{2f}(E)}{\tau_{21}} \times \frac{n_{1e}(E)}{n_1(E)} - \frac{n_{2f}(E)}{\tau_{rad}} = 0 , \tag{9}$$

$$\frac{dn_{1f}(E)}{dt} = \frac{n_{2f}(E)}{\tau_{21}} \times \frac{n_{1e}(E)}{n_1(E)} - \frac{n_{1f}(E)}{\tau_{rad}} = 0 . \tag{10}$$

The detected PL peak intensities of the ground and excited states are proportional to the values of $n_1$ and $n_2$, respectively, thus $\tau_{21}$ is determined by using (10). Combining (9) and (10) and using a value of 30 ps for the carrier capturing lifetime by QDs (Sanguinetti et al., 1999) yields the value of $\tau_{32}$. Following a similar procedure, we get the value of $g$. Use these calculated parameters, the rate-equation set (4)-(6) is solved numerically by fitting the temperature dependent integrated PL intensities of the ground state and the excited state. Once the carrier distribution functions $n_{1f}(E)$ and $n_{2f}(E)$ are determined, the PL spectra of ground state ($PL_1$) and excited state ($PL_2$) can be expressed as

$$PL_1(E) = \beta \times n_{1f}(E)/\tau_{rad} , \tag{11}$$

$$PL_2(E) = \beta \times n_{2f}(E)/\tau_{rad} , \tag{12}$$

where $\beta$ is a normalizing factor. From (11) and (12), the measured temperature dependent PL spectra of the ground state and the excited state are reproduced. The parameters used in our calculation are listed in Table 1.

| Sample | g ($s^{-1}$) | $\tau_{32}$ (ps) | $\tau_{21}$ (ps) | $\tau_{23}$ (ps) | $\tau_{34}$ (ps) |
|---|---|---|---|---|---|
| A | $1\times10^{21}$ | 14 | 68 | 0.17 | $5.5\times10^{-6}$ |
| B | | | 33 | | |
| C | | | 10 | | |

Table 1. Parameters used in the calculations of PL peak intensities and relaxation lifetimes of the samples

### 3.3 Electron-Phonon Scattering Effect

The total linewidth of PL emission in QD system can be decomposed into two components: inhomogeneous and homogeneous. The nature of these two mechanisms is totally different. Inhomogeneous broadening in the QD system arises from small fluctuations in the QDs confining size, the alloy composition variations, and the shifts due to strain-field effects (Seebeck et al., 2005; Zhao et al., 2002). The major contribution to the inhomogeneous broadening comes from the size variation due to the large confining potentials and the small volumes. We can express the inhomogeneous broadening lineshape as a Gaussian function

$$G(E) = G_0 \exp\left[\frac{-(E-E_0)^2}{2\sigma^2}\right], \tag{13}$$

where $G_0$ and $E_0$ are the amplitude and peak energy position, respectively, and $\sigma$ is the standard deviation of the distribution.

Homogeneous broadening is mainly due to the exciton-phonon interaction. Both acoustic and optical phonons are involved in the process (Ortner et al, 2004). The phonon contribution of the linewidth is proportional to phonon population density. In acoustic phonon case, such a density increases linearly with the temperature. On the other hand, optical phonons have a relatively fixed frequency. The number of phonons thermally excited follows Bose-Einstein statistics. The expression of the total homogeneous linewidth can be written as following (Christen & Bimberg, 1990)

$$\Gamma_{homo} = \gamma_{AC} T + \frac{\gamma_{LO}}{\left[\exp\left(\hbar\omega_{LO}/k_B T\right) - 1\right]}. \tag{14}$$

The first term represents the acoustic phonon contributions with proportionality constant $\gamma_{AC}$ and the second term represents the optical phonon contributions. $\gamma_{LO}$ is the longitudinal optical (LO) phonon broadening constant and $\hbar\omega_{LO}$ is the LO phonon energy. Since the phonon interactions are the results of lattice vibration, the phonon broadening(denoted as $\Gamma_{phonon}$) takes the shape of Lorentzian function (Christen & Bimberg, 1990)

$$\Gamma_{phonon}(E) = \frac{1}{(E-E_0)^2 + {\Gamma_{homo}}^2}, \tag{15}$$

where $\Gamma_{homo}$ is the homogeneous linewidth given by (14).

The electron-phonon interaction in QDs and the interaction with the wetting layer continuum act as additional sources of lineshape broadening (Sanguinetti et al., 1999). In order to include carrier-phonon interaction into the model, homogeneous energy broadening has to be considered. In QD systems, all sharp excitonic transition lines at different energies are homogeneously broadened by phonons at the same time. The total transition at each energy point is the sum of the contributions of all energy points. Thus the total lineshape of a transition involving both inhomogeneous and homogeneous broadening is the convolution of the individual lineshapes. Based on the discussion, the total transition lineshape of the energy state involving both thermal redistribution and phonon scattering of

carriers is obtained by the convolution of state distribution function and the Lorentzian function $\Gamma_{phonon}(E)$.

$$n_{1f}^{ph}(E) = \int n_{1f}(E - E')\,\Gamma_{phonon}(E')dE', \tag{16}$$

$$n_{2f}^{ph}(E) = \int n_{2f}(E - E')\,\Gamma_{phonon}(E')dE'. \tag{17}$$

Calculations of the temperature dependent FWHMs for the samples, which combine thermal redistribution and electron-phonon scattering effects, are shown in Fig. 6 with adapted values of $\gamma_{AC}$=15 $\mu$eV/K, $\gamma_{LO}$=25 meV, and $\hbar\omega_{LO}$=30 meV for InAs QDs (Gammon et al., 1995; Zhao et al., 2002). The contribution from the thermal redistribution effect on FWHM is also shown. As can be seen in this figure, the experimental data for sample A are fixed to the values obtained from the contribution of redistributed carriers at $T$<180 K, supplying the evidence of carrier redistribution in the sample. As $T$>180 K, the temperature is high enough and the electron-phonon scattering starts to come into effect. However, the

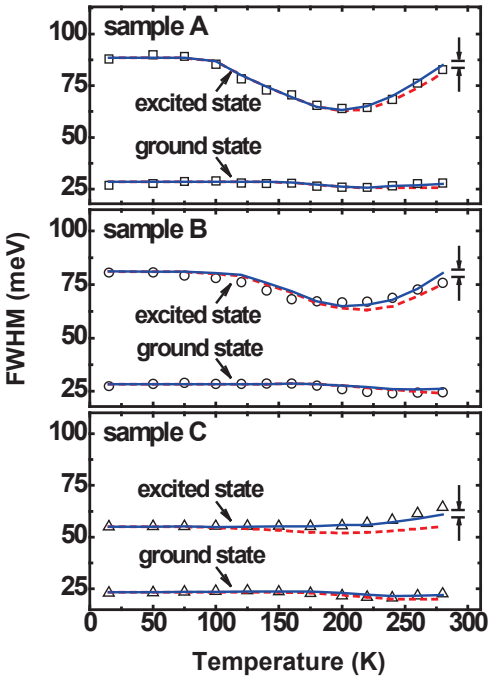


Fig. 6. Experimental and calculated FWHM of sample A, sample B, and sample C. The symbols are experimental data and the solid lines are the calculated results combining the carrier redistribution and electron-phonon scattering effects together. The dashed curves represent the contribution from thermal redistribution of carriers, compared with the linewidth resolution of 5.5 meV

effect on FWHM is unobvious and the tendency of PL linewidth with temperature is dominated by the thermal redistribution of carriers. On the other hand, referring to the simulated PL linewidth of sample C, little decrease is obtained at $T$=100-200 K in the curve which considers only the contribution of thermal redistribution. It indicates that repopulation of carriers among QDs is existent in this sample, while this phenomenon is too weak to be visible in the measured FWHMs. Joining in the electron-phonon scattering effect; the simulated FWHMs exhibit a monotonous broadening of the spectra as the temperature increases, coinciding with the experimental data.

### 3.4 Intersublevel Relaxation Process

The intersublevel relaxation lifetimes of the samples can be calculated from (2) with

$$f_1(T) = \frac{n_{1f}(E)}{n_1(E)}. \tag{18}$$

Since $f_1(T)$ is the probability of occupancy for ground state, in equilibrium condition, it is expressed as

$$f_1(T) = \frac{1}{1+\exp\left[(E_1 - E_2)/k_B T\right]}. \tag{19}$$

The relaxation lifetimes simulated by (18) for the samples, as shown in Fig. 7, are decreasing with increasing temperature. These results agree with the increase in number of phonons predicted by the Bose distribution function: $[\exp(\hbar\omega/kT)-1]^{-1}$. It is noticeable that the calculated relaxation lifetimes for sample A, sample B, and sample C at $T$=15 K are 347 ps, 160 ps, and 40 ps, respectively. Evidently, the lifetimes of sample A and sample B are much longer than that of sample C, resulting from their lower uniformity of QD structures. The shortest intersublevel relaxation times of sample C coincide with the hindered phonon bottleneck.

The corresponding values calculated from (19) of the samples at different temperatures are also shown in Fig. 7. Observing the calculated results from (18) and (19), the discrepancy between the curves is evident at lower temperature but the tendency of them becomes gradually similar as the temperature is raised up. At low temperature, the carrier recombination is much faster than the thermal emission, and the carrier distribution is non-equilibrium (Jiang & Singh, 1999). With the increase of temperature, the thermal emission time reduces and becomes smaller compared to the radiative recombination in the QD system. The carriers redistribute among different dots and thus approach to the thermal equilibrium distribution. Owing to the highest excited state energy and the smallest energy separation between the intersublevels of sample A, carriers start to thermally emit at a lower temperature than the other ones. As a result, sample A exhibits the lowest temperature where the relaxation lifetimes start approaching to the values that predicted under the thermal equilibrium condition.

Calculations of normalized PL peaks intensities of the samples are shown in Fig. 8, correlate well with the measured data. Observing the curves shown in the plot, peak intensities of ground state and excited state quench in the high temperature range because the carriers are

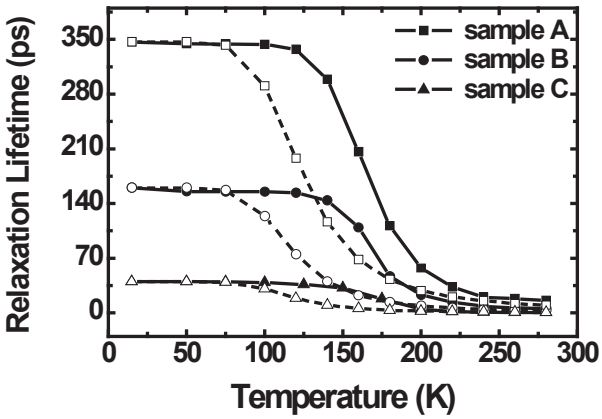


Fig. 7. Calculated intersublevel relaxation lifetimes from excited state to ground state for sample A, sample B, and sample C. The corresponding dashed lines with hollow symbols are the values that calculated under the assumption of thermal equilibrium, and normalized to the simulated relaxation lifetimes of sample A, sample B, and sample C, respectively

emitted into the GaAs barrier and irreversibly lost. We denote the temperature where the excited state starts to quench as $T_Q$. Sample A exhibits the lowest $T_Q$ (160K) and the fastest quenching rate, coinciding with its highest excited state emission energy and the smallest energy separation. The temperature $T_Q$ of sample B and sample C are 180K and 200 K, respectively. It is noticeable that the thermal quench of ground state is much slower for sample C than that for sample A and sample B. That can be explained by the different intersublevel relaxation lifetimes of the samples. The shorter relaxation lifetimes of sample C imply that the phonon bottleneck effect is partly relaxed for the sample. Through the more active phonon-assisted scatterings, more carriers relax to the ground state during the transferring process, slowing down the quenching rate of ground state.

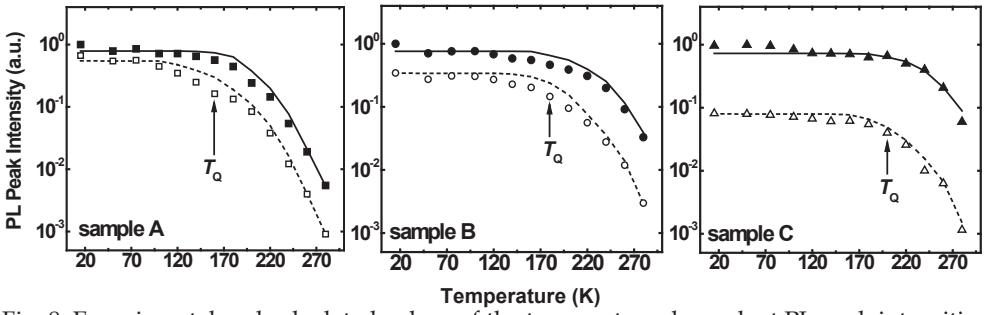


Fig. 8. Experimental and calculated values of the temperature dependent PL peak intensities of ground state and excited state of sample A, sample B, and sample C. The filled (hollow) symbols are the experimental data of ground (excited) state and the solid (dashed) lines are the calculated results of ground (excited) state. $T_Q$ denotes the temperature where the peak intensity starts to quench

The carriers transferring mechanisms are expressed more definitely in Fig. 9 by calculating the numerical values of carriers which transferring in excited state and wetting layer for sample A and sample C. A stronger dependence on temperature is obtained in Fig. 9 for sample A. According to the curves shown in the upper panel of Fig. 9(a), thermally excited carriers from QDs to wetting layer increase rapidly within the temperature range 100-200 K. At T>200 K, the number of emitting carriers saturates and then decreases. Consulting to the plot shown in the lower panel of Fig. 9(a), carriers relaxing from wetting layer to excited state also increases at *T*=100-200 K, indicating the fact of thermal redistribution of carriers. Furthermore, emitting carriers growing up as *T*>200 K, here the temperature is high enough for carriers escaping to the GaAs barrier and irreversibly lost. The thermal loss reduces the excitons in wetting layer, which in turn suppresses the carriers transferring in the excited state.

Calculation for sample C is shown in Fig. 9(b). Comparing the simulation results to that of sample A, it is clearly seen in the upper panel that the calculated radiative recombination term possesses a less important portion of the transferring carriers. The calculated result is consistent with the shorter relaxation lifetime of sample C. Because most of the injected carriers relax to the ground state, fewer carriers exist in the excited state. The thermal redistribution of carriers in the QD system is then retarded; thermal emission occurs at a higher temperature and the amount of thermally escaping excitons is smaller than that of sample A. Consequently, the simulated results exhibit a similar but weaker response to temperature change. It is obvious that the dot size uniformity of the QD systems plays an influential role in the carrier relaxation process.

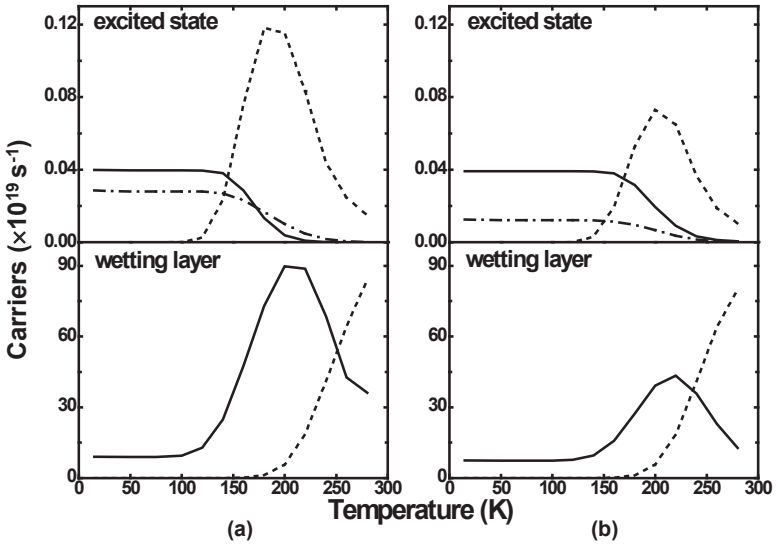


Fig. 9. Amounts of transferring carriers of each energy level in the QD system for (a) sample A, and (b) sample C. Dash-dotted lines in upper panels denote the radiative recombination terms. Solid lines and dotted lines denote the relaxation and thermal emission portions, respectively

## 4. Conclusion

In this chapter, we have investigated the effects of phonon-assisted transferring of carriers on QD system both experimentally and theoretically. The relaxation and thermal emission of carriers are analyzed quantitatively by a rate-equation model. The model is based on a set of rate equations which connect the ground state, the excited state, the wetting layer, and the GaAs barrier in the QD system. All of the important mechanisms for explaining the unique evolution of quantum dot PL spectra are taken into account, including the inhomogeneous broadening of QDs, the random population of density of states, thermal emission and retrapping, radiative and nonradiative recombination, and the electron-phonon scattering. The simulated results exhibit a good agreement to the experimental data measured from samples with different dot densities and size uniformities for temperatures ranging from 15 K to 280 K. Quantitative discussion of the carriers which thermally excited and relax between the excited state and the wetting layer provides an explicit proof of the thermal redistribution and lateral transition of carriers via the wetting layer.

The phonon-assisted activations of excitons with increasing temperatures are analyzed in detail as well. Homogeneous broadening is included in the rate equation model to demonstrate the correlation between thermal redistribution and electron-phonon scattering effects on the PL spectra of QD system and the intersublevel relaxation lifetimes is calculated. According to the theoretical analysis, carriers redistribute apparently with increasing temperature for sample with evident phonon-bottleneck effect and the effect of electron-phonon scattering is suppressed. On the other hand, the thermal redistribution effect is weak and compensated by the thermal-enhanced electron-phonon scattering for sample with relaxed phonon bottleneck and the electron-phonon scattering occupies an evident portion of the transferring mechanisms in the QD system. It is coinciding with the observed monotonic increase of FWHMs with temperature.

Furthermore, the numerical values of transferring carriers in discrete energy levels under different temperatures are also calculated. The shorter relaxation lifetime of the sample with better size-uniformity implies a restricted phonon bottleneck effect, and the unapparent change of excitons with temperature in each energy level reveals a better thermal stability. The simulation result confirms that the thermal redistribution of carriers and the electron phonon scattering affect the temperature dependent PL spectra simultaneously, and the size-uniformity of quantum dots is of essential importance for thermal activated mechanisms in quantum dot systems. Detailed investigations into the carrier dynamics in QD systems are of particular significance to the design of QD structures. Requirement of the relaxation lifetime is severe in the case of high-speed modulation. Therefore, our work has particular significance to the design of optoelectronic devices by QD structures which exhibiting truly three-dimensional confined state transitions.

## 5. Acknowledgment

This work was supported by the National Science Council of the Republic of China under Contract NSC 97-2112-M-131-001.

## 6. References


Bafna, M. K.; Sen, P. & Sen, P. K. (2006). Temperature dependence of the photoluminescence properties of self-assembled InGaAs/GaAs single quantum dot, *Journal of Applied Physics*, Vol. 100, pp. 103515

Benisty, H.; Sotomayor-Torres, C. M. & Weisbuch, C. (1991). Intrinsic mechanism for the poor luminescence properties of quantum-box systems, *Physical Review B*, Vol. 44, pp. 10945-10948

Benisty, H. (1995). Reduced electron-phonon relaxation rates in quantum-box systems: Theoretical analysis, *Physical Review B*, Vol. 51, pp. 13281-13293

Bissiri, M.; Hőgersthal, G. B. H.; Capizzi, M.; Frigeri, P. & Franchi, S. (2001). Quantum size and shape effects on the excited states of $In_xGa_{1-x}As$ quantum dots, *Physical Review B*, Vol. 64, pp. 245337

Bockelmann, U. & Bastard, G. (1990). Phonon scattering and energy relaxation in two-, one-, and zero-dimensional electron gases, *Physical Review B*, Vol. 42, pp. 8947-8951

Chang, W. H.; Hsu, T. M.; Tsai, K. F.; Nee, T. E.; Chyi, J. I. & N. T. Yeh, (1999). Excitation Density and Temperature Dependent Photoluminescence of InGaAs Self-Assembled Quantum Dots, *Japanese Journal of Applied Physics*, Vol. 38, pp. 554-557

Cheng, W. Q.; Xie, X. G.; Zhong, Z. Y.; Cai, L. H. ; Huang, Q. & Zhou, J. M. (1998). Photoluminescence from InAs quantum dots on GaAs(100), *Thin Solid Films*, Vol. 312, pp. 287-290

Christen, J. & Bimberg, D. (1990). Line shapes of intersubband and excitonic recombination in quantum wells: Influence of final-state interaction, statistical broadening, and momentum conservation, *Physical Review B*, Vol. 42, pp. 7213-7218

Dawson, P.; Rubel, O.; Baranovskii, S. D.; Pierz, K.; Thomas, P. & Göbel, E. O. (2005). Temperature-dependent optical properties of InAs/GaAs quantum dots: Independent carrier versus exciton relaxation, *Physical Review B*, Vol. 72, pp. 235301

Duarte, C. A.; Silva, E. C. F. da; Quivy, A. A.; Silva, M. J. da; Martini, S.; Leite, J. R.; Meneses, E. A. & Lauretto, E. (2003). Influence of the temperature on the carrier capture into self-assembled InAs/GaAs quantum dots, *Journal of Applied Physics*, Vol. 93, pp. 6279-6283

Gammon, D.; Rudin, S.; Reinecke, T. L.; Katzer, D. S. & Kyono, C. S. (1995). Phonon broadening of excitons in $GaAs/Al_xGa_{1-x}As$ quantum wells, *Physical Review B*, Vol. 51, pp. 16785

Giorgi, M. De; Lingk, C.; Plessen, G. von; Feldmann, J.; Rinaldis, S. De; Passaseo, A.; Vittorio, M. De; Cingolani, R. & Lomascolo, M. (2001). Capture and thermal re-emission of carriers in long-wavelength InGaAs/GaAs quantum dots, *Applied Physics Letters*, Vol. 79, pp. 3968-3970

Grosse, S.; Sandmann, J. H. H.; Plessen, G. von & Feldmann, J. (1997). Carrier relaxation dynamics in quantum dots: Scattering mechanisms and state-filling effects, *Physical Review B*, Vol. 55, pp. 4473-4476

Hai, G. Q. & Oliveira, S. S. (2006). Electron relaxation induced by electron–longitudinal-acoustic-phonon scattering in single and coupled quantum dots in external magnetic and electric fields, *Physical Review B*, Vol. 74, pp. 193303

Jiang, H & Singh, J. (1999). Nonequilibrium distribution in quantum dots lasers and influence on laser spectral output, *Journal of Applied Physics*, Vol. 85, pp. 7438-7442

Lee, J. C.; Hu, Y. J.; Wu, Y. F.; Nee, T. E.; Wang, J. C. & Fang, J. H. (2007). Intersublevel Relaxation Properties of Self-Assembled InAs/GaAs Quantum Dot Heterostructures, *Proceedings of the 7th IEEE International Conference on Nanotechnology*, pp. 934-937, Hong Kong, August 2008

Lee, H.; Yang, W. & Sercel, P. C. (1997). Temperature and excitation dependence of photoluminescence line shape in InAs/GaAs quantum-dot structures, *Physical Review B*, Vol. 55, pp. 9757-9762

Lobo, C.; Leon, R.; Marcinkevicius, S.; Yang, W.; Sercel, P. C.; Liao, X. Z.; Zou, J. & Cockayne, D. J. (1999). Inhibited carrier transfer in ensembles of isolated quantum dots, *Physical Review B*, Vol. 60, pp. 16647-16651

Malik, S.; Ru, E. C. Le; Childs, D. & Murray, R. (2001). Time-resolved studies of annealed InAs/GaAs self-assembled quantum dots, *Physical Review B*, Vol. 63, pp. 155313

Mukai, K.; Ohtsuka, N.; Shoji, H. & Sugawara, M. (1996). Phonon bottleneck in self-formed $In_xGa_{1-x}As/GaAs$ quantum dots by electroluminescence and time-resolved photoluminescence, *Physical Review B*, Vol. 54, pp. R5243-R5246

Nee, T. E.; Wu, Y. F. & Lin, R. M. (2005). Effect of carrier hopping and relaxing on photoluminescence line shape in self-organized InAs quantum dot heterostructures, *Journal of Vacuum Science & Technology B*, Vol. 23, pp. 954-958

Nee, T. E.; Wu, Y. F.; Cheng, C. C. & Shen, H. T. (2006). Carrier dynamics study of temperature and excitation dependent photoluminescence from InAs/GaAs quantum dots, *Journal of Applied Physics*, Vol. 99, pp. 013506

Ortner, G.; Yakovlev, D. R.; Bayer, M.; Rudin, S.; Reinecke, T. L.; Fafard, S.; Wasilewski, Z. & Forchel, A. (2004). Temperature dependence of the zero-phonon linewidth in InAs/GaAs quantum dots, *Physical Review B*, Vol. 70, pp. 201301

Polimeni, A.; Patanè, A.; Henini, M.; Eaves, L. & Main, P. C. (1999). Temperature dependence of the optical properties of $InAs/Al_yGa_{1-y}As$ self-organized quantum dots, *Physical Review B*, Vol. 59, pp. 5064-5068

Raymond, S.; Fafard, S.; Poole, PJ.; Wojs, A.; Hawrylak, P.; Charbonneau, S.; Leonard, D.; Leon, R.; Petroff, PM. & Merz, JL. (1996). State filling and time-resolved photoluminescence of excited states in $In_xGa_{1-x}As/GaAs$ self-assembled quantum dots, *Physical Review B*, Vol. 54, pp. 11548-11554

Sanguinetti, S.; Henini, M.; Alessi, M. G.; Capizzi, M.; Frigeri, P. & Franchi, S. (1999). Carrier thermal escape and retrapping in self-assembled quantum dots, *Physical Review B*, Vol. 60, pp. 8276-8283

Sanguinetti, S.; Watanabe, K.; Tateno, T.; Wakaki, M.; Koguchi, N.; Kuroda, T.; Minami, F. & Gurioli, M. (2002). Role of the wetting layer in the carrier relaxation in quantum dots, *Applied Physics Letters*, Vol. 81, pp. 613-615

Schmidt, K. H.; Medeiros-Ribeiro G.; Oestreich, M. & Petroff, P. M. (1996). Carrier relaxation and electronic structure in InAs self-assembled quantum dots, *Physical Review B*, Vol. 54, pp. 11346-11353

Seebeck, J.; Nielsen, T. R.; Gartner, P. & Jahnke, F. (2005). Coherent resonant tunneling time and velocity in finite periodic systems, *Physical Review B*, Vol. 71, pp. 125317

Smith, L. M.; Leosson, K.; Erland, J.; Jensen, J. R.; Hvam, J. M. & Zwiller, V. (2001). Excited State Dynamics in $In_{0.5}Al_{0.04}Ga_{0.46}As/Al_{0.08}Ga_{0.92}As$ Self-Assembled Quantum Dots, *Physica Status Solidi (b)*, Vol. 224, pp. 447-451

Solomon, G. S.; Trezza, J. A. & Harris, J. S. J. (1995). Effects of monolayer coverage, flux ratio, and growth rate on the island density of InAs islands on GaAs, *Applied Physics Letters*, Vol. 66, pp. 3161-3163

Tarasov, G. G.; Mazur, Yu. I.; Zhuchenko, Z. Ya.; Maaßdorf, A.; Nickel, D.; Tomm, J. W.; Kissel, H.; Walther, C. & Masselink, W. T. (2000). Carrier transfer in self-assembled coupled InAs/GaAs quantum dots, *Journal of Applied Physics*, Vol. 88, pp. 7162-7170

Tomm, J. W.; Mazur, Y. I.; Tarasov, G. G.; Zhuchenko, Z. Y.; Kissel, H.; Masselink, W. T. & Elsaesser, T. (2003). Transit luminescence of dense InAs/GaAs quantum dot arrays, *Physical Review B*, Vol. 67, pp. 045326

Wu, Y. F.; Lee, J. C. & Hu, Y. J. (2008). Effect of Phonon-assisted Transferring of Excitons on Photoluminescence Spectra from InAs Quantum Dots, *Proceedings of 2008 International Electron Devices and Materials Symposia*, pp. 676-679, Taiwan, November 2008

Xu, Z. Y.; Lu, Z. D.; Yang, X. P.; Yuan, Z. L.; Zheng, B. Z.; Xu, J. Z.; Ge, W. K.; Wang, Y.; Wang, J. & Chang, L. L. (1996). Carrier relaxation and thermal activation of localized excitons in self-organized InAs multilayers grown on GaAs substrates, *Physical Review B*, Vol. 54, pp. 11528-11531

Yang, W.; Lowe-Webb, R. R.; Lee, H. & Sercel, P. C. (1997). Effect of carrier emission and retrapping on luminescence time decays in InAs/GaAs quantum dots, *Physical Review B*, Vol. 56, pp. 13314-13320

Zhang, X. Q.; Ganapathy, S.; Kumano, H.; Uesugi, K. & Suemene, I. (2002). Photoexcited carrier transfer in InGaAs quantum dot structures: Dependence on the dot density, *Journal of Applied Physics*, Vol. 92, pp. 6813-6818

Zhao, H.; Wachter, S. & Kalt, H. (2002). Effect of quantum confinement on exciton-phonon interactions, *Physical Review B*, Vol. 66, pp. 085337

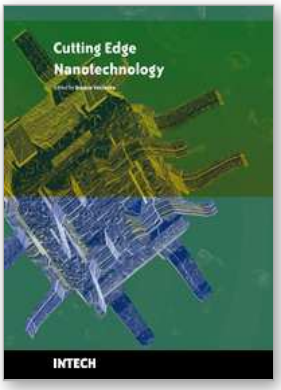


**Cutting Edge Nanotechnology**

Edited by Dragica Vasileska

ISBN 978-953-7619-93-0
Hard cover, 444 pages
**Publisher** InTech
**Published online** 01, March, 2010
**Published in print edition** March, 2010

The main purpose of this book is to describe important issues in various types of devices ranging from conventional transistors (opening chapters of the book) to molecular electronic devices whose fabrication and operation is discussed in the last few chapters of the book. As such, this book can serve as a guide for identifications of important areas of research in micro, nano and molecular electronics. We deeply acknowledge valuable contributions that each of the authors made in writing these excellent chapters.

**How to reference**

In order to correctly reference this scholarly work, feel free to copy and paste the following:

Jiunn-Chyi Lee and Ya-Fen Wu (2010). Intersublevel Relaxation Properties of Self- Assembled InAs/GaAs Quantum Dot Heterostructures, Cutting Edge Nanotechnology, Dragica Vasileska (Ed.), ISBN: 978-953-7619-93-0, InTech, Available from: http://www.intechopen.com/books/cutting-edge-nanotechnology/intersublevel-relaxation-properties-of-self-assembled-inas-gaas-quantum-dot-heterostructures

INTECH
open science | open minds

**InTech Europe**
University Campus STeP Ri
Slavka Krautzeka 83/A
51000 Rijeka, Croatia
Phone: +385 (51) 770 447
Fax: +385 (51) 686 166
www.intechopen.com

**InTech China**
Unit 405, Office Block, Hotel Equatorial Shanghai
No.65, Yan An Road (West), Shanghai, 200040, China
中国上海市延安西路65号上海国际贵都大饭店办公楼405单元
Phone: +86-21-62489820
Fax: +86-21-62489821